

This document is the accepted manuscript version of the following article:

C. Wäckerlin, F. Donati, A. Singha, R. Baltic, S. Rusponi, K. Diller, F. Patthey, M. Pivetta, Y. Lan, S. Klyatskaya, M. Ruben, H. Brune, J. Dreiser

**Giant Hysteresis of Single-Molecule Magnets Adsorbed on a Nonmagnetic Insulator**

Advanced Materials, 2016, 28, 5195–5199

<https://dx.doi.org/10.1002/adma.201506305>

**Giant Hysteresis of Single-Molecule Magnets Adsorbed on a Nonmagnetic Insulator**

by *Christian Wäckerlin, Fabio Donati, Aparajita Singha, Romana Baltic, Stefano Rusponi, Katharina Diller, François Patthey, Marina Pivetta, Yanhua Lan, Svetlana Klyatskaya, Mario Ruben, Harald Brune and Jan Dreiser\**

[\*] Dr. Jan Dreiser  
Swiss Light Source, Paul Scherrer Institut  
CH-5232 Villigen PSI (Switzerland)  
E-mail: [jan.dreiser@psi.ch](mailto:jan.dreiser@psi.ch)

Dr. Christian Wäckerlin, Dr. Fabio Donati, Mrs. Aparajita Singha, Ms. Romana Baltic, Dr. Stefano Rusponi, Dr. Katharina Diller, Dr. François Patthey, Prof. Harald Brune, Dr. Jan Dreiser

Institute of Condensed Matter Physics (ICMP), Ecole Polytechnique Fédérale de Lausanne (EPFL)

Station 3, CH-1015 Lausanne (Switzerland)

Dr. Marina Pivetta

Institute of Physics (IPHY), Ecole Polytechnique Fédérale de Lausanne (EPFL)

Station 3, CH-1015 Lausanne (Switzerland)

Dr. Yanhua Lan, Dr. Svetlana Klyatskaya, Prof. Mario Ruben  
Institute of Nanotechnology, Karlsruhe Institute of Technology (KIT)  
D-76344 Eggenstein-Leopoldshafen (Germany)

Prof. Mario Ruben  
Institut de Physique et Chimie des Matériaux (IPCMS), Université de Strasbourg  
F-67034 Strasbourg (France)

Keywords: Single-Molecule Magnets, Surfaces, X-ray Absorption Spectroscopy, Scanning Tunneling Microscopy

Single-molecule magnets (SMMs)<sup>[1]</sup> are very promising for molecular spintronics<sup>[2]</sup> and quantum information processing,<sup>[3]</sup> because of their magnetic bistability and the quantum nature of their spin. The first step towards devices based on SMMs is their adsorption onto electrode surfaces.<sup>[4,5]</sup> However, already this step represents a serious obstacle as it severely compromises the magnetic remanence.<sup>[6–12]</sup> Here, we solve this problem by introducing a tunnel barrier between the SMMs and the metal electrode. For TbPc<sub>2</sub> SMMs<sup>[13,14]</sup> on MgO on Ag(100) we demonstrate record values of the magnetic remanence and the hysteresis opening, outperforming any previously reported surface adsorbed SMMs.

The two key properties of a magnet relevant to devices are large remanence and wide hysteresis opening. Achieving these goals represents a largely unresolved challenge for SMMs adsorbed at surfaces. The molecule-surface interaction leads to a significant shrinking of the remanence and the hysteresis<sup>[7,12]</sup> all the way to their complete disappearance.<sup>[6,7]</sup>

Current strategies to overcome this problem are to exploit weak adsorption, *e.g.* on graphite,<sup>[8,9]</sup> or decoupling from the surface by long chemical linkers<sup>[4,5,15]</sup> or bulky ligands.<sup>[11]</sup> Despite that, so far all attempts to enhance the vanishingly small magnetic remanence of SMMs on surfaces have failed.<sup>[4-12]</sup> Consequently, the magnetic remanence of surface adsorbed SMMs lags far behind the benchmark set by bulk samples<sup>[16]</sup>, which are, however, not useful for device applications.

Here we introduce an entirely different strategy, namely the insertion of a tunnel barrier between the SMMs and the metal electrode. We use MgO, well-known in inorganic spintronic applications,<sup>[17,18]</sup> which allows to control the electron tunneling rate over many orders of magnitude.<sup>[19]</sup> Moreover, we employ the TbPc<sub>2</sub> SMM<sup>[13,14,20-23]</sup> as a model system. In the neutral molecule, the Tb(III) ion exhibits an electronic spin state of  $J = 6$ . It is sandwiched between two phthalocyanine (Pc) macrocycles (*cf.* schematic view in **Figure 1a**) hosting an unpaired electron delocalized over the Pc ligands. The magnetic anisotropy imposes an energy barrier of  $\sim 65$  meV for magnetization reversal,<sup>[23]</sup> which is largest within the whole series of lanthanide-Pc<sub>2</sub> SMMs.<sup>[13]</sup> On nonmagnetic conducting substrates, only vanishing remanence and very narrow hysteresis loops were observed, much smaller than in bulk measurements,<sup>[20]</sup> illustrating the disruptive effects of the surface.<sup>[6-9]</sup> We note that the adsorption of TbPc<sub>2</sub> on (anti)ferromagnetic materials represents a different situation because of the magnetic exchange interaction with the substrate.<sup>[24,25]</sup> In that case, the SMMs were not shown to exhibit slow relaxation of magnetization. Rather, the hysteresis is linked to the one of the magnetic substrates, *i.e.*, it is not an intrinsic property of the SMMs. Overall, the detailed

knowledge on TbPc<sub>2</sub> makes it an ideal candidate to test if a tunnel barrier can boost the magnetic properties of surface-adsorbed SMMs. In this communication we show that the magnetic remanence and hysteresis opening obtained with TbPc<sub>2</sub> on MgO tunnel barriers outperform the ones of any other surface adsorbed SMM<sup>[4–12,15,26]</sup> as well as those of bulk samples of TbPc<sub>2</sub>.<sup>[20]</sup>

The scanning tunneling microscopy (STM) images in Figure 1b and c show that TbPc<sub>2</sub> self-assembles by forming perfectly ordered two-dimensional islands on two monolayers (MLs) of MgO on Ag(100). In line with former results, the SMMs are adsorbed flat on the surface (*cf.* discussion of our STM and XLD data below).<sup>[6,27]</sup> This excludes that the extraordinary magnetic properties observed in this study are due to upstanding molecules having their macrocycles perpendicular to the surface, which would lead to a reduced interaction of the Tb(III) ion with the surface. The high-resolution image in Figure 1c reveals eight lobes per molecule, reminiscent of the staggered conformation of the two phthalocyanine ligands.<sup>[27]</sup> Islands with identical molecular assembly are formed by TbPc<sub>2</sub> adsorbed directly onto Ag(100), as shown in the Supporting Information.

The magnetic properties of the Tb ions in the surface-adsorbed SMMs are determined by X-ray magnetic circular dichroism (XMCD) measurements at the M<sub>4,5</sub> (3d → 4f) edges of Tb. For sub-MLs of TbPc<sub>2</sub> on MgO we find a strong remanence larger than 40 % of the saturation magnetization  $M_{\text{sat}}$  and a hysteresis opening up to 3 T at 3 K (Figure 1d). These values vastly exceed the corresponding records reported for any surface-adsorbed SMM<sup>[4–11,15,26]</sup> as well as the ones reported for bulk TbPc<sub>2</sub>.<sup>[20]</sup> The large remanence indicates that quantum tunneling of magnetization is strongly suppressed for fields below 3 T, with only a very subtle modulation of the relaxation rate across the hysteresis loop.

The effect of the tunnel barrier becomes evident when comparing with TbPc<sub>2</sub> directly adsorbed onto Ag(100) where the hysteresis opening is barely visible. In fact, the area of the opening has decreased by a factor of 10 (Figure 1e). The large opening of sub-MLs on

MgO/Ag(100) is also reduced in TbPc<sub>2</sub> multilayers (Figure 1e). This is attributed to magnetic interactions between the molecules.<sup>[21]</sup> In addition to MgO we also investigated hexagonal boron nitride (*h*-BN)<sup>[28]</sup> as a tunnel barrier. The hysteresis opening on *h*-BN is wider than the one reported for most surface-adsorbed TbPc<sub>2</sub> (Supporting Information), however, it is significantly narrower than on the MgO thin film. MgO is more efficient in suppressing electron scattering from the substrate as it can be grown in multilayers, while *h*-BN forms a self-limiting monolayer.

The electronic ground state and magnetic moments of the Tb ion, as well as the molecular orientation are inferred from the X-ray absorption spectra and their circular (XMCD) and linear (XLD) dichroism (**Figure 2**). XLD, which is directly sensitive to the molecular orientation, evidences that the molecules adsorb with the same orientation on MgO (Figure 2) and on Ag(100) (Supporting Information). This is in line with our STM results (Figure 1b and c and Figures S1-S3) showing that the TbPc<sub>2</sub> macrocycles are parallel to the surfaces of MgO and Ag(100). Furthermore, our results are consistent with XLD spectra of TbPc<sub>2</sub> on metal surfaces reported in the literature.<sup>[6,7]</sup> The same orientation is also observed for TbPc<sub>2</sub> on *h*-BN and for the multilayer (Supporting Information). The Tb spin and orbital magnetic moments extracted from the XMCD spectra (*cf.* Supporting Information) are in excellent agreement with previous studies of TbPc<sub>2</sub> on metal surfaces<sup>[6,7]</sup> and on graphite.<sup>[8,9]</sup> Therefore the larger remanence is neither due to a different magnetic ground state of the Tb ion nor to strong modifications in the magnetic anisotropy.

To determine the magnetic relaxation times of TbPc<sub>2</sub>/MgO we have performed time dependent XMCD measurements at 0.5 T after saturating the magnetization at 4 T (**Figure 3**). The magnetization *vs* time traces  $M(t)$  decay exponentially (Figure 3a). This decay with rate  $\tau^{-1}$  becomes faster with increasing X-ray flux. Therefore intrinsic relaxation (rate  $\tau_i^{-1}$ ) and photon-induced demagnetization (rate  $\tau_{ph}^{-1}$ )<sup>[29]</sup> coexist. The respective rates add up yielding the decay rate  $\tau^{-1} = \tau_i^{-1} + \tau_{ph}^{-1}$ . Consistently, the fit  $\tau(\Phi)^{-1} = \tau_i^{-1} + \sigma\Phi$  in Figure 3b

shows that the decay rates are linear with the X-ray flux  $\Phi$  within the error bars. The intercept at zero X-ray flux yields the intrinsic relaxation time  $\tau_i = 14_{-4}^{+10}$  min at 0.5 T, and the slope  $\sigma = 0.21 \pm 0.05 \text{ nm}^2 = (2.1 \pm 0.5) \times 10^9$  barn is the cross section of the photon-induced demagnetization process. The asymptotic values of the magnetization decrease with increasing X-ray flux  $\Phi$ , indicating that the X-ray induced demagnetization drives the magnetization to a value which is lower than the thermodynamic equilibrium at 0.5 T, in contrast to the intrinsic relaxation. Notably, the demagnetization is not a result of simple spatially homogeneous heating or radiation damage (*cf.* Supporting Information).

Temperature dependent hysteresis loops of TbPc<sub>2</sub>/MgO (**Figure 4**) evidence slow relaxation of the magnetization beyond 6 K. In fact, the hysteresis area still exhibits a finite value at 8 K, which is the highest blocking temperature ever reported for surface adsorbed SMMs.

We rationalize the large magnetic remanence and the wide hysteresis opening of TbPc<sub>2</sub> on MgO by identifying two key aspects. These are, first, the strong suppression of scattering of conduction electrons from the metal at the molecule and, second, the low molecule-surface hybridization. The electron tunneling rate depends exponentially on the barrier thickness. For MgO tunnel barriers it is reduced by a factor of  $\sim 3 \times 10^3$  per nanometer ( $\sim 5$  ML MgO).<sup>[30]</sup> In accordance, narrower hysteresis loops are observed for thinner MgO and for *h*-BN monolayers (*cf.* Supporting Information).

Regarding the second key aspect, bulk studies have shown that the preservation of the ideal  $D_{4d}$  symmetry is important to achieve long relaxation times and large coercive fields in TbPc<sub>2</sub>.<sup>[21,22]</sup> Symmetry breaking enables mixing terms in the TbPc<sub>2</sub> spin Hamiltonian that, together with the hyperfine interaction, promote quantum tunneling of magnetization especially around zero field.<sup>[4,21,22]</sup> Owing to the low hybridization on MgO the upper and lower Pc ligands retain the same electronic structure as in the gas phase, preserving the molecular  $D_{4d}$  symmetry nearly perfectly. In contrast, upon direct adsorption onto metal surfaces the electronic structure of the lower Pc ligand in contact with the surface is slightly

altered because of adsorption bonds and molecule–surface charge transfer, reducing the symmetry of the Tb ligand field to  $C_{4v}$  or lower. Thus symmetry breaking of the ligand field, presumably together with electron scattering, leads to the barely open hysteresis loops of TbPc<sub>2</sub> on Ag(100) in this work and on Au(111)<sup>7</sup>, and to the closed loop on Cu(100).<sup>[6]</sup> Graphite is weakly hybridizing, however, it does not suppress electron scattering leading to narrow hysteresis openings as well.<sup>[8,9]</sup>

Concerning magnetic interactions between adjacent molecules, for sub-monolayers of TbPc<sub>2</sub> we observe a negligible influence of the molecular coverage on the hysteresis opening (Supporting Information). Together with the 2D molecular self-assembly seen by STM, this implies that lateral magnetic interactions are insignificant. On the contrary, our data on TbPc<sub>2</sub> multilayers on MgO reveal that vertical interactions accelerate magnetization relaxation.<sup>[20,21]</sup> In summary, we have demonstrated that MgO thin films realize the combination of efficient protection from electron scattering and weak molecule-surface hybridization to achieve optimal properties of SMMs on electrode surfaces. In addition, in the present case of TbPc<sub>2</sub> the molecules are self-assembled into well-ordered islands leading to highly uniform molecular ensembles with out-of-plane easy axes. Epitaxial MgO layers promote a very large tunnel magneto-resistance in inorganic devices based on ferromagnetic electrodes.<sup>[31]</sup> Therefore the combination of SMMs and epitaxial MgO tunnel junctions opens up a path towards SMM based tunnel devices.

### *Experimental*

*Sample preparation:* The Ag(100) single crystal substrate was prepared by repeated cycles of sputtering with Ar<sup>+</sup> ions and annealing. The epitaxial MgO layers were grown by sublimation of Mg in O<sub>2</sub> atmosphere (10<sup>-6</sup> mbar) while keeping the sample at 500 K.<sup>[19]</sup> A submonolayer of TbPc<sub>2</sub> was sublimed at 650 K at a rate of ~0.1 ML/min onto the surface kept at room

temperature. The multilayer sample was prepared by sublimation of ~3 ML of TbPc<sub>2</sub> onto MgO/Ag(100).

*X-ray absorption spectroscopy:* The X-ray absorption experiments were performed at the EPFL/PSI X-Treme beamline<sup>[32]</sup> at the Swiss Light Source at a temperature of 3 K in total electron yield mode using circularly ( $\sigma^+$ ,  $\sigma^-$ ) and linearly polarized ( $\sigma^h$ ,  $\sigma^v$ ) X-rays with the magnetic field applied parallel to the X-ray beam. XMCD and XLD spectra correspond to the differences, ( $\sigma^+ - \sigma^-$ ) and ( $\sigma^v - \sigma^h$ ), respectively. The X-ray flux was measured with a photodiode located after the last optical element of the beam line and is given in units of  $\Phi_0 = 0.034 \text{ photons nm}^{-2} \text{ s}^{-1}$  (*cf.* extended methods in Supporting Information).

#### *Acknowledgements*

C.W., A.S., R.S., and J.D. gratefully acknowledge funding by the Swiss National Science Foundation (C.W. & J.D. grant no. PZ00P2\_142474). K.D. acknowledges support from the ‘EPFL Fellows’ program co-funded by Marie Curie, FP7 grant agreement no. 291771. Y.L. and M.R. would like to thank the EC-FET-Open project “MOQUAS”.

((Supporting Information is available online from Wiley InterScience or from the author)).

Received: ((will be filled in by the editorial staff))

Revised: ((will be filled in by the editorial staff))

Published online: ((will be filled in by the editorial staff))

#### *References*

- [1] R. Sessoli, D. Gatteschi, A. Caneschi, M. A. Novak, *Nature* **1993**, 365, 141.
- [2] M. Urdampilleta, S. Klyatskaya, J.-P. Cleuziou, M. Ruben, W. Wernsdorfer, *Nat. Mater.* **2011**, 10, 502.
- [3] S. Thiele, F. Balestro, R. Ballou, S. Klyatskaya, M. Ruben, W. Wernsdorfer, *Science* **2014**, 344, 1135.
- [4] M. Mannini, F. Pineider, P. Saintavit, C. Danieli, E. Otero, C. Sciancalepore, A. M. Talarico, M.-A. Arrio, A. Cornia, D. Gatteschi, R. Sessoli, *Nat. Mater.* **2009**, 8, 194.
- [5] M. Mannini, F. Pineider, C. Danieli, F. Totti, L. Sorace, P. Saintavit, M.-A. Arrio, E. Otero, L. Joly, J. C. Cezar, A. Cornia, R. Sessoli, *Nature* **2010**, 468, 417.
- [6] S. Stepanow, J. Honolka, P. Gambardella, L. Vitali, N. Abdurakhmanova, T.-C. Tseng, S. Rauschenbach, S. L. Tait, V. Sessi, S. Klyatskaya, M. Ruben, K. Kern, *J. Am. Chem. Soc.* **2010**, 132, 11900.
- [7] L. Margheriti, D. Chiappe, M. Mannini, P.-E. Car, P. Saintavit, M.-A. Arrio, F. B. de Mongeot, J. C. Cezar, F. M. Piras, A. Magnani, E. Otero, A. Caneschi, R. Sessoli, *Adv. Mater.* **2010**, 22, 5488.

- [8] M. Gonidec, R. Biagi, V. Corradini, F. Moro, V. De Renzi, U. del Pennino, D. Summa, L. Muccioli, C. Zannoni, D. B. Amabilino, J. Veciana, *J. Am. Chem. Soc.* **2011**, *133*, 6603.
- [9] D. Klar, A. Candini, L. Joly, S. Klyatskaya, B. Krumme, P. Ohresser, J.-P. Kappler, M. Ruben, H. Wende, *Dalton Trans* **2014**, *43*, 10686.
- [10] J. Dreiser, *J. Phys. Condens. Matter* **2015**, *27*, 183203.
- [11] L. Malavolti, V. Lanzilotto, S. Ninova, L. Poggini, I. Cimatti, B. Cortigiani, L. Margheriti, D. Chiappe, E. Otero, P. Sainctavit, F. Totti, A. Cornia, M. Mannini, R. Sessoli, *Nano Lett.* **2015**, *15*, 535.
- [12] R. Westerström, A.-C. Uldry, R. Stania, J. Dreiser, C. Piamonteze, M. Muntwiler, F. Matsui, S. Rusponi, H. Brune, S. Yang, A. Popov, B. Büchner, B. Delley, T. Greber, *Phys. Rev. Lett.* **2015**, *114*, 087201.
- [13] N. Ishikawa, M. Sugita, T. Ishikawa, S. Koshihara, Y. Kaizu, *J. Am. Chem. Soc.* **2003**, *125*, 8694.
- [14] N. Ishikawa, *Polyhedron* **2007**, *26*, 2147.
- [15] M. Mannini, F. Bertani, C. Tudisco, L. Malavolti, L. Poggini, K. Misztal, D. Menozzi, A. Motta, E. Otero, P. Ohresser, P. Sainctavit, G. G. Condorelli, E. Dalcanale, R. Sessoli, *Nat. Commun.* **2014**, *5*, 4582.
- [16] J. D. Rinehart, M. Fang, W. J. Evans, J. R. Long, *Nat. Chem.* **2011**, *3*, 538.
- [17] X. Jiang, R. Wang, R. M. Shelby, R. M. Macfarlane, S. R. Bank, J. S. Harris, S. S. P. Parkin, *Phys. Rev. Lett.* **2005**, *94*, 056601.
- [18] I. G. Rau, S. Baumann, S. Rusponi, F. Donati, S. Stepanow, L. Gragnaniello, J. Dreiser, C. Piamonteze, F. Nolting, S. Gangopadhyay, O. R. Albertini, R. M. Macfarlane, C. P. Lutz, B. A. Jones, P. Gambardella, A. J. Heinrich, H. Brune, *Science* **2014**, *344*, 988.
- [19] S. Schintke, S. Messerli, M. Pivetta, F. Patthey, L. Libioulle, M. Stengel, A. De Vita, W.-D. Schneider, *Phys. Rev. Lett.* **2001**, *87*, 276801.
- [20] M. Gonidec, E. S. Davies, J. McMaster, D. B. Amabilino, J. Veciana, *J. Am. Chem. Soc.* **2010**, *132*, 1756.
- [21] L. Malavolti, M. Mannini, P.-E. Car, G. Campo, F. Pineider, R. Sessoli, *J. Mater. Chem. C* **2013**, *1*, 2935.
- [22] N. Ishikawa, M. Sugita, W. Wernsdorfer, *Angew. Chem. Int. Ed.* **2005**, *44*, 2931.
- [23] F. Branzoli, P. Carretta, M. Filibian, M. J. Graf, S. Klyatskaya, M. Ruben, F. Coneri, P. Dhakal, *Phys. Rev. B* **2010**, *82*, 134401.
- [24] A. Lodi Rizzini, C. Krull, T. Balashov, J. J. Kavich, A. Mugarza, P. S. Miedema, P. K. Thakur, V. Sessi, S. Klyatskaya, M. Ruben, S. Stepanow, P. Gambardella, *Phys. Rev. Lett.* **2011**, *107*, 177205.
- [25] A. Lodi Rizzini, C. Krull, T. Balashov, A. Mugarza, C. Nistor, F. Yakhov, V. Sessi, S. Klyatskaya, M. Ruben, S. Stepanow, P. Gambardella, *Nano Lett.* **2012**, *12*, 5703.
- [26] J. Dreiser, C. Wäckerlin, M. E. Ali, C. Piamonteze, F. Donati, A. Singha, K. S. Pedersen, S. Rusponi, J. Bendix, P. M. Oppeneer, T. A. Jung, H. Brune, *ACS Nano* **2014**, *5*, 4662.
- [27] T. Komeda, H. Isshiki, J. Liu, Y.-F. Zhang, N. Lorente, K. Katoh, B. K. Breedlove, M. Yamashita, *Nat. Commun.* **2011**, *2*, 217.
- [28] S. Joshi, F. Bischoff, R. Koitz, D. Ecija, K. Seufert, A. P. Seitsonen, J. Hutter, K. Diller, J. I. Urgel, H. Sachdev, J. V. Barth, W. Auwärter, *ACS Nano* **2014**, *8*, 430.
- [29] J. Dreiser, R. Westerström, C. Piamonteze, F. Nolting, S. Rusponi, H. Brune, S. Yang, A. Popov, L. Dunsch, T. Greber, *Appl. Phys. Lett.* **2014**, *105*, 032411.
- [30] A. Zaleski, J. Wrona, M. Czapkiewicz, W. Skowroński, J. Kanak, T. Stobiecki, *J. Appl. Phys.* **2012**, *111*, 033903.
- [31] S. Yuasa, A. Fukushima, H. Kubota, Y. Suzuki, K. Ando, *Appl. Phys. Lett.* **2006**, *89*, 042505.



- [32] C. Piamonteze, U. Flechsig, S. Rusponi, J. Dreiser, J. Heidler, M. Schmidt, R. Wetter, M. Calvi, T. Schmidt, H. Pruchova, J. Krempasky, C. Quitmann, H. Brune, F. Nolting, *J. Synchrotron Radiat.* **2012**, *19*, 661.

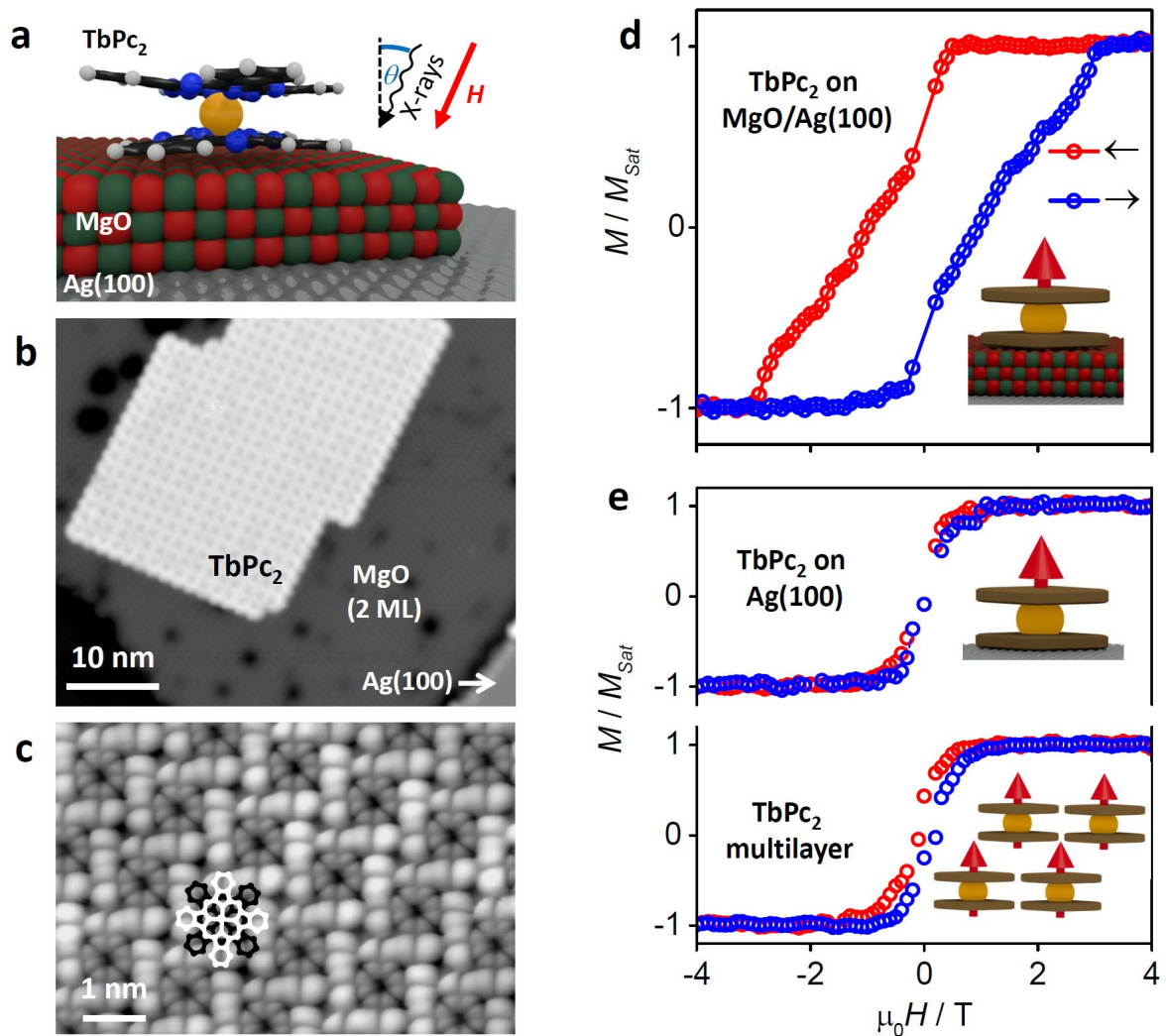


**Figure 1.** Self-assembly and exceptional magnetic remanence and hysteresis of TbPc<sub>2</sub> molecules on insulating MgO films. (a) Sketch of a TbPc<sub>2</sub> molecule on an ultrathin MgO film on Ag(100). (b, c) Scanning tunnelling microscopy images revealing self-assembled arrays of TbPc<sub>2</sub> on 2 monolayers (MLs) of MgO. The image sizes and parameters (scale bar, bias voltage, current setpoint) are (10 nm, +2 V, 20 pA) for b) and (1 nm, -2 V, 20 pA) for c), respectively. (d, e) Hysteresis loops obtained with XMCD at 3 K for 0.6 ML TbPc<sub>2</sub> on 5 ML MgO compared with 0.3 ML TbPc<sub>2</sub> adsorbed directly on Ag(100) and with a TbPc<sub>2</sub> multilayer (3 ML) on MgO (field sweep rate 2 T/min, normal incidence, X-ray flux 0.25  $\Phi_0$  (d) and  $\Phi_0$  (e), respectively).

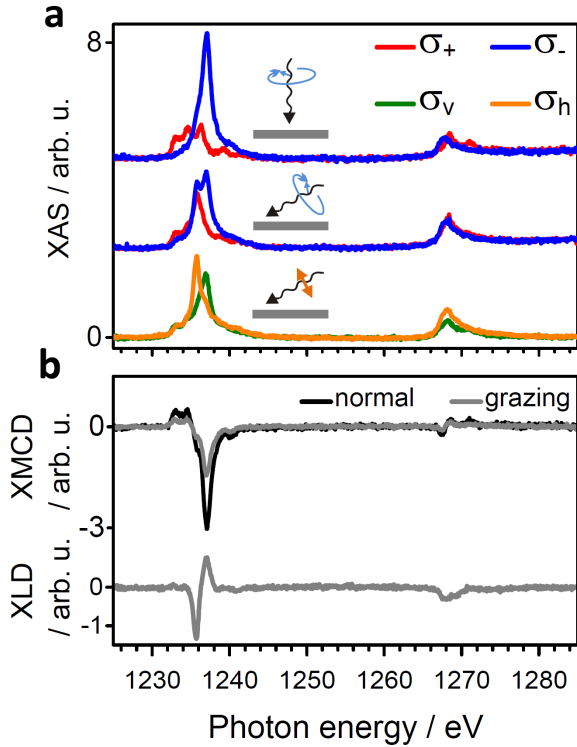


**Figure 2.** X-ray spectra of a submonolayer of TbPc<sub>2</sub> on MgO revealing the magnetic anisotropy and the orientation of the molecules. XAS at the Tb M<sub>4,5</sub> edges acquired at 3 K using circularly (σ<sub>+</sub>, σ<sub>-</sub>) and linearly (σ<sub>h</sub>, σ<sub>v</sub>) polarized light. The same arbitrary units are used in a) and b). (a) The spectra with circularly polarized X-rays were obtained in normal (θ = 0°) and grazing (θ = 60°) incidence in an applied magnetic field of 6.8 T. (b) Their difference, XMCD, is a direct measure of the magnetic moment of Tb. The peak XMCD-to-XAS ratio (σ<sup>+</sup> - σ<sup>-</sup>)/(σ<sup>+</sup> + σ<sup>-</sup>) is -80% and -55% for normal and grazing incidence, respectively. The X-ray linear dichroism (XLD), the difference of the linearly polarized XAS, is obtained at 50 mT in grazing incidence, with the strongest XLD-to-XAS-ratio of -45%.

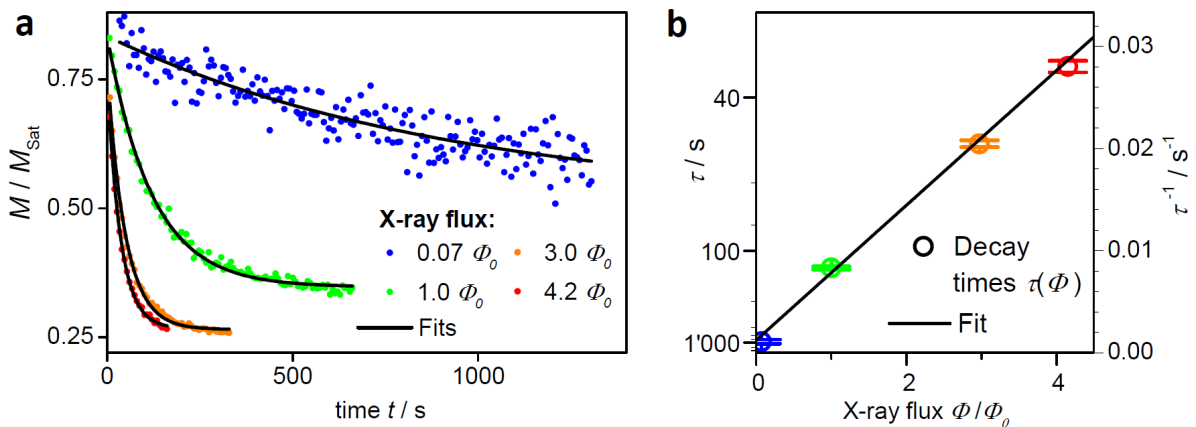


**Figure 3.** Intrinsic relaxation and X-ray induced demagnetization. The time dependent XMCD signal was obtained at 0.5 T after magnetizing the samples at 4 T and switching on the X-ray beam at time  $t = 0$ , immediately after reaching 0.5 T. (a) With increasing X-ray flux  $\Phi$ , the magnetization  $M$  decays faster. The exponential fits yield the decay times  $\tau$  of the

magnetization as a function of X-ray flux  $\Phi$ . (b) The intercept yields the intrinsic relaxation time  $\tau_i = 14_{-4}^{+10}$  min.

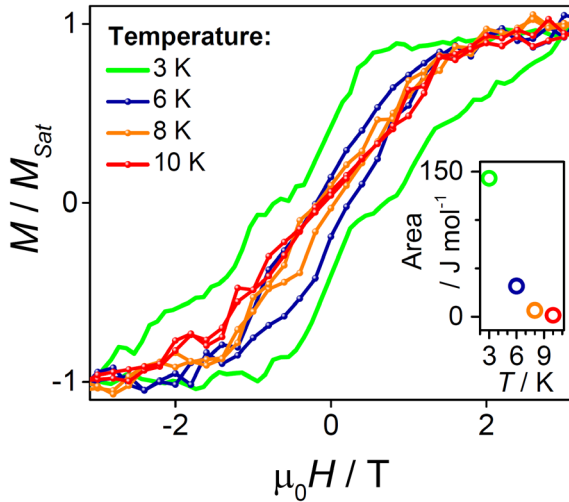


**Figure 4.** Temperature dependent magnetization curves of  $\text{TbPc}_2/\text{MgO}/\text{Ag}(100)$ . With increasing temperature the magnetization loop gradually closes until the hysteresis fully vanishes at 10 K (X-ray flux  $\Phi_0$ , 0.3 ML  $\text{TbPc}_2$  on 4.8 ML  $\text{MgO}$ ). The area of the hysteresis opening is plotted in the inset.

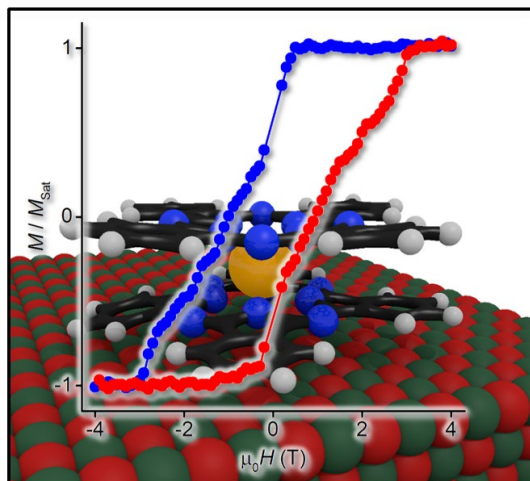
*ToC entry*

We demonstrate that TbPc<sub>2</sub> single-molecule magnets (SMMs) adsorbed on a magnesium oxide tunnel barrier exhibit record magnetic remanence, record hysteresis opening, perfect out-of-plane alignment of the magnetic easy axes and self-assembly into a well-ordered layer.

Keywords: Single-Molecule Magnets, Surfaces, X-ray Absorption Spectroscopy, Scanning Tunneling Microscopy

by *Christian Wäckerlin, Fabio Donati, Aparajita Singha, Romana Baltic, Stefano Rusponi, Katharina Diller, François Patthey, Marina Pivetta, Yanhua Lan, Svetlana Klyatskaya, Mario Ruben, Harald Brune and Jan Dreiser\**

### **Giant Hysteresis of Single-Molecule Magnets Adsorbed on a Tunnel Barrier**



ToC figure ((55 mm broad, 50 mm high, or 110 mm broad, 20 mm high))